

Document Version

Final published version

Citation (APA)

Lu, G., van Driel, W. D. (Ed.), Fan, X., Fan, J., & Zhang, G. Q. (2018). LED-Based Luminaire Color Shift Acceleration and Prediction. In W. D. van Driel, X. Fan, & G. Q. Zhang (Eds.), *Solid State Lighting Reliability Part 2: Components to Systems* (1 ed., pp. 201-219). (Solid State Lighting Technology and Application Series; Vol. 3). Springer.
https://doi.org/10.1007/978-3-319-58175-0_9

Important note

To cite this publication, please use the final published version (if applicable).
Please check the document version above.

Copyright

In case the licence states "Dutch Copyright Act (Article 25fa)", this publication was made available Green Open Access via the TU Delft Institutional Repository pursuant to Dutch Copyright Act (Article 25fa, the Taverne amendment). This provision does not affect copyright ownership.
Unless copyright is transferred by contract or statute, it remains with the copyright holder.

Sharing and reuse

Other than for strictly personal use, it is not permitted to download, forward or distribute the text or part of it, without the consent of the author(s) and/or copyright holder(s), unless the work is under an open content license such as Creative Commons.

Takedown policy

Please contact us and provide details if you believe this document breaches copyrights.
We will remove access to the work immediately and investigate your claim.

Chapter 9

LED-Based Luminaire Color Shift Acceleration and Prediction

Guangjun Lu, Willem Dirk van Driel, Xuejun Fan, Jiajie Fan,
and Guo Qi Zhang

Abstract Color stability is of major concern for LED-based products. Currently, much effort is done on lumen maintenance, and for color shift, no agreed method currently exists, be it from testing or from prediction side. To investigate the physics of color shift, we present experiments of each individual part failure of each individual part that are present in LED-based products. In order to develop a color shift prediction method, it is imperative to investigate the color shift contribution by each individual part. We present a new method to predict color shift on a system level, which we named the *view factor approach*. We compare this

G. Lu (✉)

Beijing Research Centre, Delft University of Technology, Beijing, China

EEMCS Faculty, Delft University of Technology, Delft, The Netherlands

State Key Laboratory of Solid State Lighting, Changzhou, China

e-mail: lv-guangjun@163.com

W.D. van Driel

Philips Lighting, High Tech Campus, Eindhoven, The Netherlands

Delft University of Technology, EEMCS Faculty, Delft, The Netherlands

e-mail: W.D.vanDriel-1@tudelft.nl

X. Fan

State Key Laboratory of Solid State Lighting, Changzhou, China

Department of Mechanical Engineering, Lamar University, Beaumont, TX 77710, USA

e-mail: xuejun.fan@lamar.edu

J. Fan

Beijing Research Centre, Delft University of Technology, Beijing, China

State Key Laboratory of Solid State Lighting, Changzhou, China

College of Mechanical and Electrical Engineering, Hohai University, Changzhou, China

e-mail: jay.fan@connect.polyu.hk

G.Q. Zhang

EEMCS Faculty, Delft University of Technology, Delft, The Netherlands

Institute of Semiconductors, Chinese Academy of Sciences, Beijing, Haidian, China

e-mail: g.q.zhang@tudelft.nl

prediction method with experiments on luminaire level to conclude that we have taken satisfactory first steps in the field of color shift predictions for LED-based systems.

9.1 Introduction

Luminous flux maintenance and color stability are two important factors to evaluate the lighting quality. While much research efforts have been done on the former and even some standards have been generated for lumen decay acceleration, research activities and achievements on the latter have lagged behind [1–3]. With increased adoption and accumulation of hours of use, awareness is growing that color shift is an issue for some products, especially in some important application fields, such as museums, patient examination rooms, urban scene illumination occasions, offices, street lighting, and so on [4, 5].

DOE Energy Star Program requires that the change of chromaticity over the lifetime of the product should be within 0.007 on the CIE 1976 (u', v') diagram [6]. Unlike traditional lighting products, the color shift mechanism of LED lighting is complex due to its much more comprehensive structure, generally composed of LED die, phosphor, silicone, reflector, diffusers, and so on, all of which may contribute to the color shift during operation, and each individual component has its own degradation mechanism [7]. Some studies have been done on some failure mechanisms of package level color shift, such as color shift to the blue end of spectrum caused by phosphor settle for the combination of “blue” LED and “yellow” phosphor, color shift caused by the discoloration of the plastic (PPA) or polycarbonate (PC) used in the package, color shift toward yellow end resulting from mean free path of the blue photons through the phosphor increase caused by delamination, and so on [8–17]. Mehr et al. experimentally investigated the color shift of remote phosphor plates made from Bisphenol-A polycarbonate (BPA-PC) and some other materials [18–21]. However, studies on the LED-based luminaire level color shift reliability are little publicly available except some based on the statistical (data-driven) method. This chapter will investigate LED-based luminaire level color shift mechanisms based on a breakdown method and introduce a novel approach for investigation of color shift contribution by each individual component. Finally, we propose a color shift acceleration and prediction approach.

9.2 Breakdown Method for Color Shift and Mechanism Investigation

9.2.1 *Materials and Methods*

A commercially widely used downlight with size of 4 in, power of 10 W, correlated color temperature (CCT) of 4000 k, was chosen as a representative, as shown in Fig. 9.1.

Fig. 9.1 Representative of downlight for color shift investigation

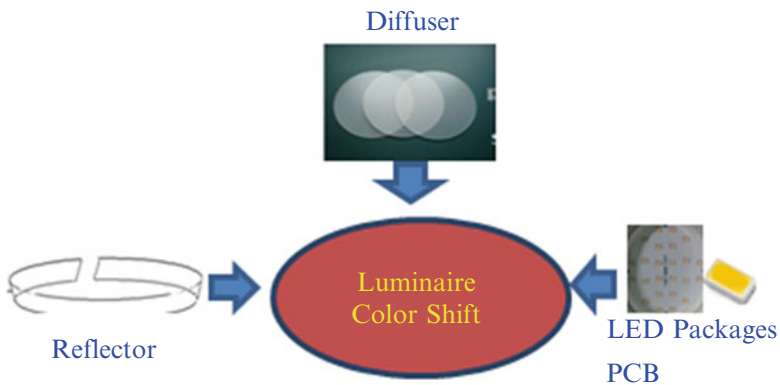


Fig. 9.2 Breakdown of downlight color shift

In terms of color shift in the study, an entire downlight can be divided into three individual parts, reflectors, diffusers, and LED packages. The color shift of each individual part adds up to the color shift of the entire downlight. Such a breakdown method can be simplified as shown in Fig. 9.2.

In the investigation, diffuser material used in the downlight is PMMA, which is widely used in indoor lighting application due to comparatively low cost and mature manufacturing process. Reflective material for the reflector is the novel microcellular PET material. Compared with the traditional metal-based reflective material, the microcellular PET has many advantages, such as high total reflectivity, high diffuse reflectivity, and lightweight. LED package is the mid-power 5630 which has comparatively high luminous efficiency and is flexible in combination for downlight application. Figures 9.3 and 9.4 show the molecular structures of PMMA and PET materials, respectively.

To investigate the physics of color shift failure of each individual part, experiments were done as follows.

Rectangular pure PMMA plates with a thickness of 3 mm and dimension of 30 mm × 50 mm and rectangular microcellular PET reflective sheets with a thickness of 0.51 mm and the same dimension of 30 mm × 50 mm were subjected to the following three experimental conditions, respectively: (1) Thermal aging in an

Fig. 9.3 Molecular structure of PMMA

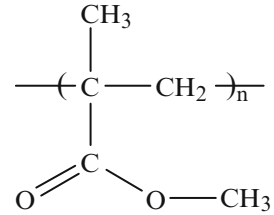
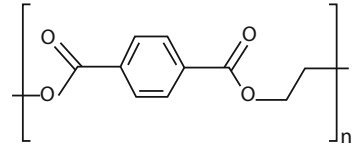


Fig. 9.4 Molecular structure of PET



aging test oven with a temperature setting of 85 °C for more than 3000 h; (2) Blue light irradiation at 85 °C for more than 3000 h (The specimens were placed inside the oven at 85 °C and exposed to blue light through the oven glass window generated by the blue light LEDs outside the oven). The wavelength of blue light used is 450 nm, the distance between blue light source and the specimens is 40 cm, and the blue light intensity that the specimen received is around 40 k lux; (3) Humidity reliability test (Specimens were put in the isothermal oven for more than 3000 h at 85 °C and 85% RH). In addition, PMMA specimens of the same type and thickness with a dimension of 100 mm × 100 mm were put separately in two ovens with a temperature of 100 °C for 3000 h and 150 °C for 360 h, respectively.

While subjected to the aging conditions: room temperature, 85 °C and 85 °C and 85% RH, the LED packages were separately mounted to small hexagonal heat sink plates and lighted up via a jig with the same current as that normally used in the downlight luminaire.

Transmittance spectra of PMMA plates and reflectance spectra of microcellular PET specimens with different aging conditions were recorded in the range 380–740 nm with a step of 5 nm with the Lambda 950 spectrophotometer (PerkinElmer 950). Relative reflectance mode other than the absolute mode is chosen to do the measurement with a universal reflectance accessory as the light spectral reference.

Stress-strain curves were also measured with a DMA Q800 to characterize the mechanical properties of Microcellular PET specimens with different aging conditions. Infrared spectra of specimens were measured for chemical analysis in the range of 900–1800 cm⁻¹ using a Perkin–Elmer Spectrum 100 series spectrometer in the attenuated total reflection (ATR) mode for 180 scans at a resolution of 5 cm⁻¹.

In addition, in order to quantify the color shift effects of microcellular PET specimens after aging, a downlight LED luminaire was used and measured by an integrating sphere with a diameter of 2 m at 2 pi mode. The LED packages subjected to different aging conditions for a different aging time were also measured by another integrating sphere with a diameter of 0.5 m at 2 pi mode too. For more details, please refer to [22–25].

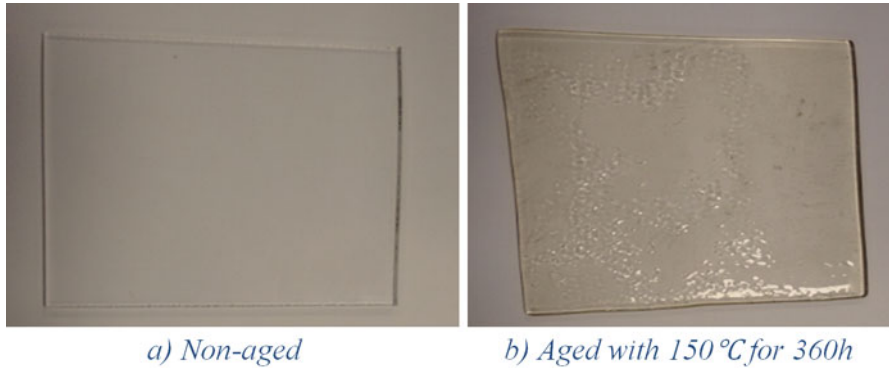


Fig. 9.5 Discoloration of PMMA after aging. (a) Nonaged. (b) Aged with 150 °C for 360 h

9.2.2 Results and Discussions

9.2.2.1 PMMA

Discoloration was not observed for any sample subjected to aging of 85 °C for 5000 h, or with additional blue light irradiation for 5000 h, or with additional humidity of 85%RH for 5000 h, or even with aging of 100 °C for 3000 h. By contrast, after 360 h of thermal aging at 150 °C in the oven, the color in the surface of PMMA specimen tends to be slightly yellowing. Pictures of the specimen before and after aging are shown in Fig. 9.5.

Note that the aging temperature 150 °C is above T_g (around 110 °C) and below melting point (around 200 °C) of the PMMA material, and we didn't observe any color change of the surface during the first day of aging.

Transmittance spectra of PMMA under different aging conditions were also measured. The transmittance of specimen aged at 150 °C for 360 h is lower than that of any subjected to other aging conditions in the wavelength range from 360 to 760 nm, and the specimens subjected to other aging conditions have almost the same spectra as that of the nonaged specimen. Furthermore, as shown in Fig. 9.7, the transmittance reduction (calculated on the difference of transmittance between lines of nonaged and aged at 150 °C shown in Fig. 9.6) of the specimen aged at 150 °C is wavelength dependent, and the reduction of transmittance at around 450 nm (blue light area) is much higher than that at around 590 nm (yellow light area) (Fig. 9.7).

FTIR analysis implies oxidation occurred to that specimen. There are three steps involved in the aging. The first step is the splitting off of the acrylate group, whereas the second step is the actual oxidation and followed by hydrogenation. Such chemical mechanism can be described in Fig. 9.8.

It should be pointed out here the experiments found that PMMA will exhibit yellowing only at high temperatures (150 °C) which are well above the glass transition temperature of the polymer. This temperature is also above the accepted

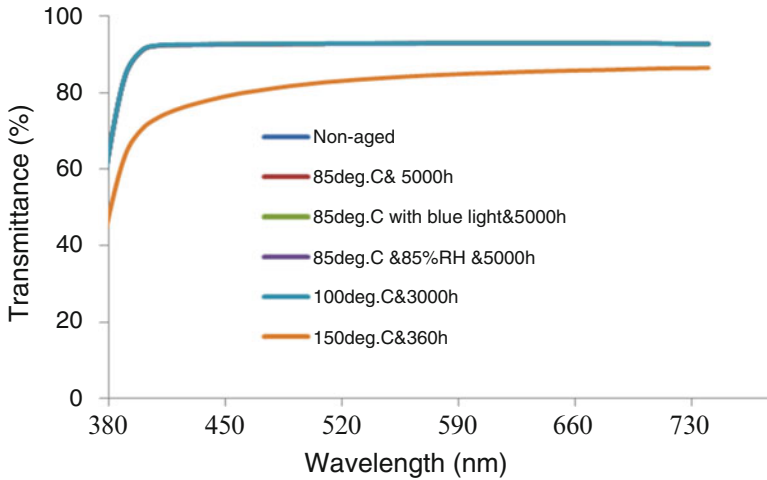


Fig. 9.6 Transmission spectra after being subjected to different aging conditions (Note: the 85 °C and 100 °C lines coincide with the nonaged line)

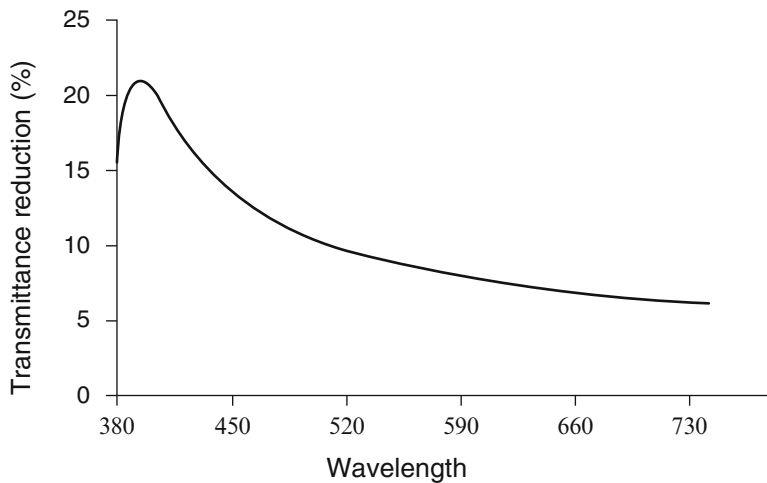


Fig. 9.7 Transmittance reduction for the PMMA subjected to 150 °C for 360 h

use temperature of PMMA and is unlikely to be used in a practical luminaire. Therefore, the risks on introducing a new failure mode is high since the experiments were performed above T_g and chain mobility will be increased.

The nonuniform reduction of transmittance in the transmission spectrum caused by aging could induce the change of radiant flux intensity ratio of blue light to yellow light, which gives rise to the color shift in perception and chromaticity change in the CIE1976 diagram. In order to quantify color shift effects of the specimen subjected to 150 °C for 360 h, as aforementioned, a downlight LED

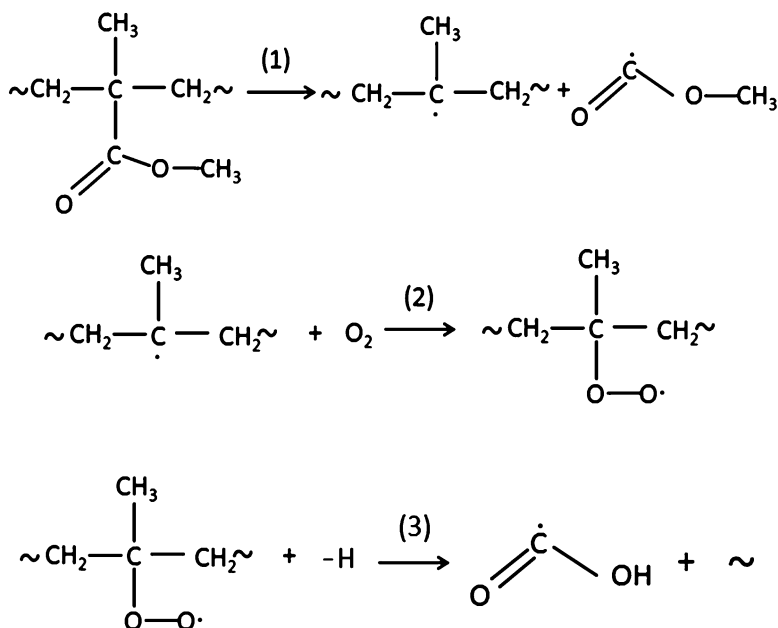


Fig. 9.8 Chemical mechanisms of oxidation and hydrogenation during aging

luminaire mounted with such an aged sample and a nonaged one of identical size was measured by an integrating sphere. Normalized spectral power distributions are shown in Fig. 9.9.

The results of color coordinates in the CIE1976 diagram by such measurement are also given, as shown in Fig. 9.10. As can be found in Fig. 9.9, the peak wavelength neither at blue light area (around 450 nm) nor at yellow light area (around 590 nm) changed; however, the peak intensity at blue light area has a more severe reduction than that at the yellow light area, which causes the reduction of radiant flux intensity ratio of blue light to yellow light and hence induces the color shift to yellow as confirmed in Fig. 9.10.

9.2.2.2 Microcellular PET

After 4000 h of aging for the microcellular PET reflective material, discoloration was not observed to any specimen. However, during manually handling when we took out the samples from the humidity test oven, one specimen broke. Hence, the stress-strain measurement was conducted on all the specimens to investigate the possible changes of mechanical property. Only the sample subjected to humidity test fractured, and this fracture occurred at a strain of 0.38% (1.1 Mpa). The samples of the nonaged and 4000 h thermally aged did not fracture during the test. The reflectance spectra of specimens after 4000 h of aging were measured and recorded

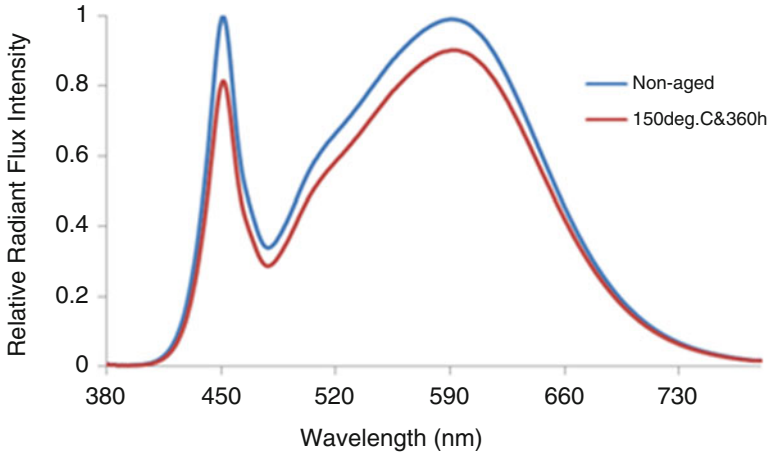


Fig. 9.9 SPDs of LED-based luminaire mounted with aged PMMA specimen

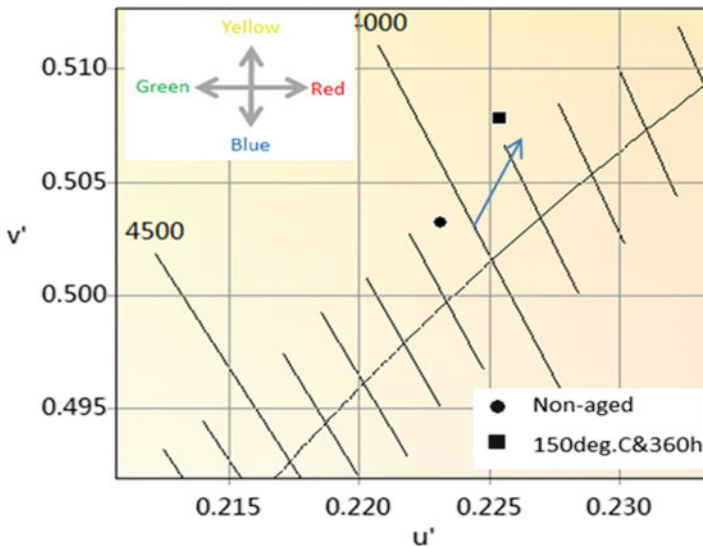


Fig. 9.10 Color coordinates in the CIE 1976 Diagram for the LED-based luminaire mounted with PMMA specimens

by a Lambda 950 spectrophotometer in a wavelength range from 380 to 800 nm with a step of 5 nm. Reflectance spectra of microcellular PET with different aging conditions are shown in Fig. 9.11. The reflectance spectrum of the 85 °C aged specimen is nearly the same as that exposed to additional blue light irradiation. Furthermore, the reflectance spectrum of the 85 °C aged specimen is higher than the nonaged one in the wavelength range from 380 to 430 nm. The specimen which was

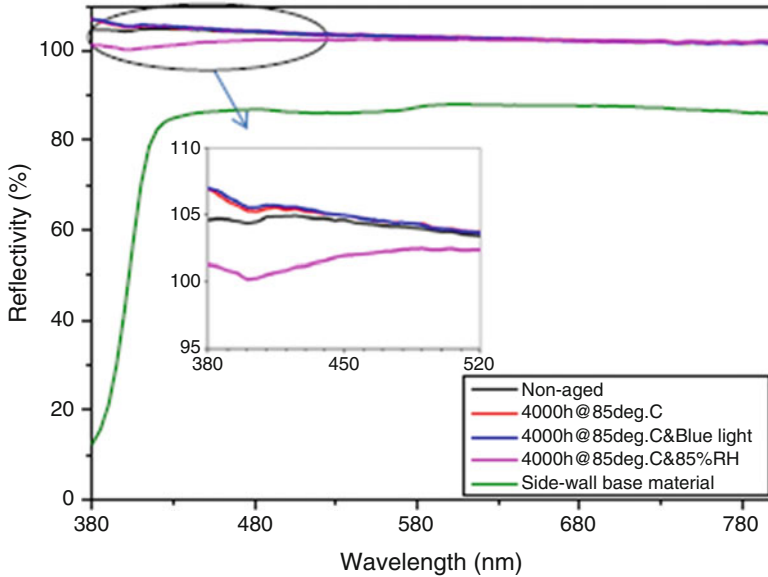


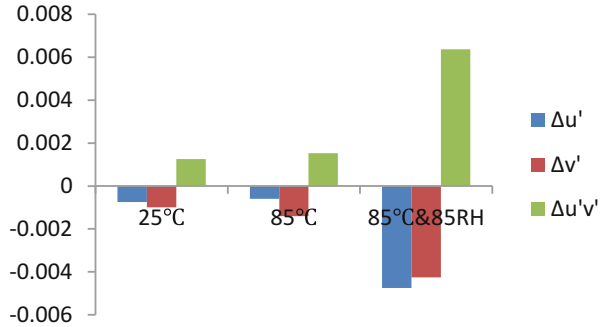
Fig. 9.11 Reflectance spectra of microcellular PET with different aging conditions and side-wall base material

subjected to humidity test has an obvious reflectivity decrease in the range from 380 to 520 nm compared to the nonaged sample.

FTIR studies were performed in order to chemically explain the abovementioned optical and mechanical property changes after aging. Compared to the slower oxidation in the thermal aging test, the hydrolytic degradation in the humidity test induces chemical structure change of the specimen, which causes the remarkable changes of optical and mechanical properties.

In order to quantify color shift effects of those specimens after aging under different conditions, a downlight LED luminaire with aged and nonaged specimens was measured by an integrating sphere, respectively. The specimen subjected to 4000 h of thermally aged test has a color shift of 0.0001 due to a reduction of u' by 0.0001, while 4000 h of humidity test causes a color shift of 0.0004 with an equivalent reduction of u' and v' of 0.0003, which is far less than 0.001 (or 1 sdcm). Note that embrittlement of the microcellular PET after 4000 h of humidity test will make it so fragile that when it is disturbed (e.g., for repair or ceiling maintenance), the material may crumble exposing the underlying paint reflector. Consequently, during the color shift investigation for 4000 h of humidity test, the microcellular PET was not mounted, during which the side-wall base material, which has a lower reflectivity, acted as a reflector. Color shift by PET was attributed to the change of flux intensity ratio of blue light to yellow light, similar to the PMMA.

Fig. 9.12 Color shift of LED packages subjected to different aging conditions



9.2.2.3 LED Package

Color data of 5630 LED packages which were subjected to different aging conditions have been measured. Color shift results ($\Delta u'$, $\Delta v'$, $\Delta u'v'$) of the specimen subjected to different aging conditions for ~6000 h were shown in Fig. 9.12. First 2000 h of data was not used due to unstable degradation. It can be found that the specimen after humidity aging test has the maximum color shift $\Delta u'v'$, and the color shift tends to blue light area for both thermal aging conditions and humidity test. Some studies implied that the moisture entrapment to the inside of silicone bulk caused a localized extremely high temperature (around 300 °C), which accelerates the degradation of LED package.

As a summary, in the color shift study, the downlight can be divided into three parts, the diffuser, the reflector, and the LED packages, which have different color shift failure physics or mechanisms and contribute differently to the total color shift. Optical properties will be changed under thermal aging conditions, which will contribute color shift for diffuser and reflectors. LED packages have a color shift toward blue during thermal aging and humidity test. Humidity test demonstrates a strong acceleration in color shift.

9.3 A Novel Approach for Color Shift Investigation on LED-Based Luminaires

9.3.1 Materials and Methods

In order to develop the color shift acceleration and prediction method, it is important to investigate the color shift contribution by each individual part. Hence, a novel approach for color shift investigation based on view factor method was proposed in this section. The downlight to be investigated was aged at 85 °C in an oven and lighted on for around 4000 h. Measured the soldering temperature T_s is around 105 °C with a thermal couple. To quantify the color and lumen change of the

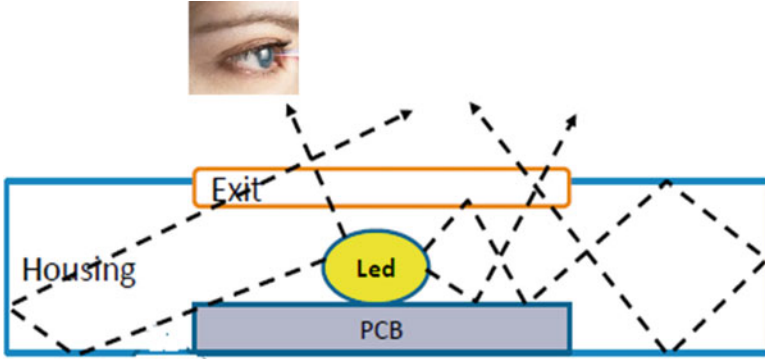


Fig. 9.13 Schematic diagrams of light paths

LED packages mounted in the downlight during aging, same type of LED packages also from same suppliers was separately mounted and placed in the same oven and lighted on with equivalent current. The T_s of LED package measured is also around $105\text{ }^\circ\text{C}$. The light flux, color, and SPDs (spectrum power distributions) of those LED packages were measured and recorded by an integrating sphere before and after aging. The diffuser used in the downlight is a type of commercial misty PMMA with a thickness of 2 mm. The transmittances of diffuser before and after aging were measured. The reflective material used in the downlight is one type of commercial PET, whose reflectivity before and after aging were also measured. Refer to [26] for more details.

To help illustrate this approach, a schematic diagram of light paths for the downlight investigated is shown in Fig. 9.13. Each exchange of light in the light paths can be considered as a contribution to color shift. The matrix Eq. 9.1 shown below can be used to describe the exchange.

$$\begin{pmatrix} \Phi_{itoLEDs} \\ \Phi_{itopcb} \\ \Phi_{itohousing} \\ \Phi_{itoexit} \end{pmatrix} = \begin{pmatrix} F_{L-L} & F_{P-L} & F_{h-L} & F_{e-L} \\ F_{L-P} & F_{P-P} & F_{h-p} & F_{e-p} \\ F_{L-h} & F_{P-h} & F_{h-h} & F_{e-h} \\ F_{L-e} & F_{P-e} & F_{h-e} & F_{e-e} \end{pmatrix} \begin{pmatrix} \Phi_{ifromLEDs} \\ \Phi_{ifrompcb} \\ \Phi_{ifromhousing} \\ \Phi_{ifromexit} \end{pmatrix} \quad (9.1)$$

Where Φ stands for the light flux and the number i denotes the number of reflections undergone. F is the so-called view factor (conservation of light: sum of each matrix column =1). The software LightTools is used to extract the view factor F and light flux Φ . For the physics of reflection, it can be described as the Eq. 9.2:

$$\begin{pmatrix} \Phi_{i+1fromLEDs} \\ \Phi_{i+1frompcb} \\ \Phi_{i+1fromhousing} \\ \Phi_{i+1fromexit} \end{pmatrix} = \begin{pmatrix} R_L & & & \\ & R_P & & \\ & & R_h & \\ & & & R_e \end{pmatrix} \begin{pmatrix} \Phi_{itoLEDs} \\ \Phi_{itopcb} \\ \Phi_{itohousing} \\ \Phi_{itoexit} \end{pmatrix} \quad (9.2)$$

Each reflection is accompanied with a small color change $\Delta u'_i, \Delta v'_i$, depending on part L, p, h , and e .

The equation for the exit transmission can be described in Eq. 9.3, as shown below. It also accompanies with a small color change during transmission. Φ_{toexit} is the light flux to exit for transmission, which can be calculated via Eq. 9.4:

$$\begin{aligned} \Phi_{\text{fromexit}} &= (1 - R_e - A)\Phi_{\text{toexit}} \\ \Phi_{\text{toexit}} &= \sum_i \Phi_{\text{itoeexit}} \end{aligned} \quad (9.3)$$

$$\begin{aligned} &= F_{L-e} \sum_i \Phi_{\text{ifromLEDs}} + F_{h-e} \sum_i \Phi_{\text{ifromhousing}} + F_{p-e} \sum_i \Phi_{\text{ifrompcb}} \\ &\quad + F_{e-e} \sum_i \Phi_{\text{ifromexit}} \end{aligned} \quad (9.4)$$

Color shift $\Delta u', \Delta v', \Delta u'v'$ of the flux to exit Φ_{toexit} in the downlight could be estimated via below Eqs. 9.5, 9.6, and 9.7. $\Delta u'_L, \Delta u'_p, \Delta u'_h$, and $\Delta u'_e$ denote the color changes of fluxes exchanged on the part L, p, h , and e . r is the ratio of the flux returned to the exit after a cycle of reflections in the downlight. All of them could also be captured by Monte Carlo simulation with the software LightTools. The color change caused by the transmission of exit diffuser can be also got via Monte Carlo simulation.

$$\Delta u' = w_{\text{LED}} \cdot \Delta u'_L + w_{\text{pcb}} \cdot \Delta u'_p + w_{\text{housing}} \cdot \Delta u'_h + w_{\text{housing}} \cdot \Delta u'_e \quad (9.5)$$

$$\Delta v' = w_{\text{LED}} \cdot \Delta v'_L + w_{\text{pcb}} \cdot \Delta v'_p + w_{\text{housing}} \cdot \Delta v'_h + w_{\text{housing}} \cdot \Delta v'_e \quad (9.6)$$

$$\Delta u'v' = \sqrt{(\Delta u')^2 + (\Delta v')^2} \quad (9.7)$$

Where $w_{\text{LED}}, w_{\text{pcb}}, w_{\text{housing}}$ and w_{exit} could be described as below:

$$\begin{aligned} w_{\text{LED}} &= \frac{F_{L-e} \sum_i \Phi_{\text{ifromLEDs}}}{\Phi_{\text{toexit}}} \\ w_{\text{pcb}} &= \frac{F_{p-e} \sum_i \Phi_{\text{ifrompcb}}}{\Phi_{\text{toexit}}} \\ w_{\text{housing}} &= \frac{F_{h-e} \sum_i \Phi_{\text{ifromhousing}}}{\Phi_{\text{toexit}}} \\ w_{\text{exit}} &= \frac{r \sum_{i-1} \Phi_{\text{ifromexit}}}{\Phi_{\text{toexit}}} \end{aligned}$$

To perform the simulations for extraction, initial condition is shown in equation:

$$\begin{pmatrix} \Phi_{0\text{fromLEDs}} \\ \Phi_{0\text{frompcb}} \\ \Phi_{0\text{fromhousing}} \\ \Phi_{0\text{fromexit}} \end{pmatrix} = \begin{pmatrix} \Phi_{\text{LEDs}} \\ 0 \\ 0 \\ 0 \end{pmatrix} \tag{9.8}$$

Some assumptions were made as follows. The LED is top emitting, and light exits from LEDs, and there is no bouncing back and forth from them.

9.3.2 Results and Discussions

9.3.2.1 Measured Results for Color Shift of Downlights After Aging

The SPD, lumen, and color data of the downlight before and after aging were measured and recorded by an integrating sphere with a diameter of 2 m at 2 pi mode. Figure 9.14 shows the SPD of the downlight before and after aging. Obvious degradation of the flux intensity could be found both in the yellow light area (around 590 nm) and blue light area (around 450 nm). Table 9.1 shows the lumen and color changes for this downlight.

Fig. 9.14 SPDs of downlight before and after aging

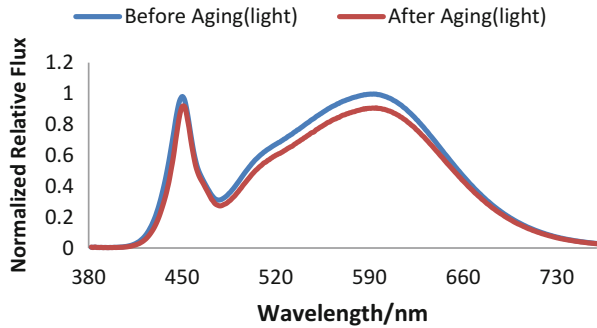


Table 9.1 Lumen and color data measurement before and after aging

			Before aging	After aging
Power		(W)	10.1	10.1
Luminous flux		[lm]	936.65	838.66
Lumen degradation		[-]	10.46%	
Color point	u'	[-]	0.2229	0.2248
	v'	[-]	0.5026	0.5041
Color shift	$\Delta u'$	[-]	0.0019	
	$\Delta v'$	[-]	0.0015	
	$\Delta u'v'$	[-]	0.0024	

Fig. 9.15 SPDs for LED packages before and after temperature aging

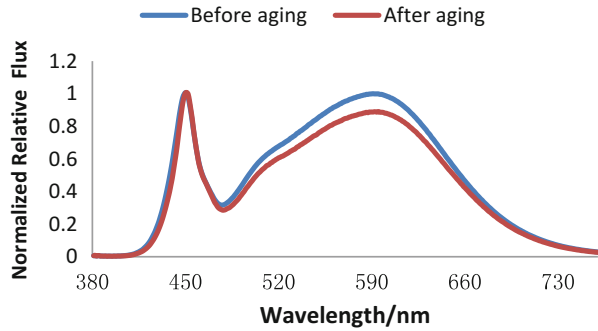


Fig. 9.16 Transmittance measured for PMMA diffuser before and after aging

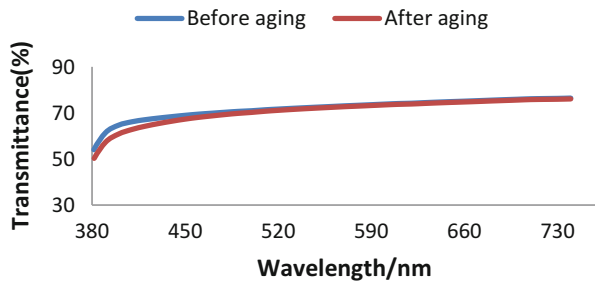
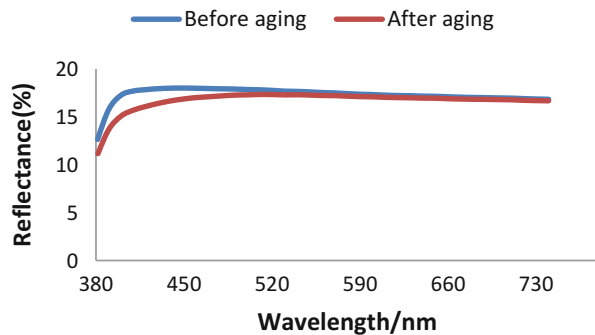


Fig. 9.17 Reflectance measured for PMMA diffuser before and after aging



9.3.2.2 Inputs for Simulation

The averages of SPDs for LED packages before and after aging are shown in Fig. 9.15, which will be used as inputs for simulation.

Both the transmittance and reflectance before and after aging were measured for the diffuser, shown in Figs. 9.16 and 9.17, respectively, which will be used as input for simulation.

PET was not only mounted on the side-wall used as the housing reflective material but also covered the PCB surface. So the housing and PCB's contribution on the color shift depends on the change of PET's reflectance. Figure 9.18 shows the reflectance measurement before and after aging, which will be used as inputs for simulation.

Fig. 9.18 Reflectance measured for PET material before and after aging

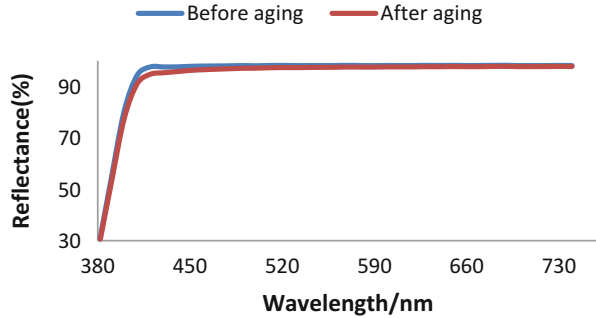
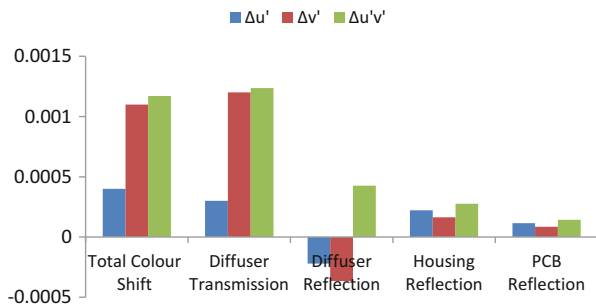


Table 9.2 View factor Table for 0 h

		From			
		LEDs	PCB	Housing	Exit
To	LEDs	0.00000	0.00000	0.00000	0.00000
	PCB	0.00000	0.00000	0.24526	0.53365
	Housing	0.21378	0.21378	0.00000	0.46635
	Exit	0.78622	0.78622	0.75474	0.00000

Fig. 9.19 Color shift of downlight at 0 h



9.3.2.3 Color Shift Results

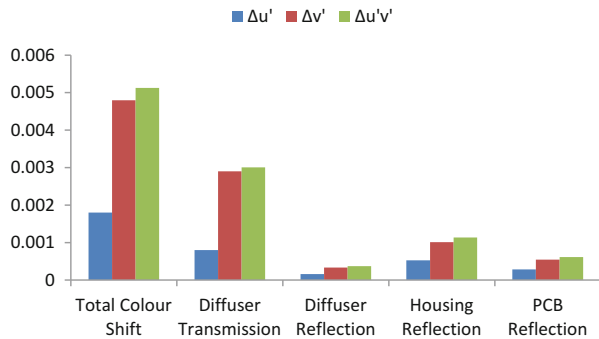
1. *Color shift before aging (0 h).*

View factors were extracted by Monte Carlo simulation as shown in Table 9.2 for the downlight before aging. Color shift of each individual part could be also got via simulation. Accordingly, the color shift of downlight could be calculated. Figure 9.19 shows the color shift of downlight at 0 h and contribution by each individual part. Even nonaged (at 0 h), the light coming out of the downlight has a color change of ~0.001 compared with the color of light emitted from the LED packages. The diffuser has a major contribution. When the light goes through the diffuser, the ratio of blue light to yellow light in the SPD has a change due to the transmittance difference between wavelengths, which leads to the color change.

Table 9.3 View factor Table for 4000 h

$t = 4000 \text{ h}$		From			
		LEDs	PCB	Housing	Exit
To	LEDs	0.00000	0.00000	0.00000	0.00000
	PCB	0.00000	0.00000	0.23939	0.53598
	Housing	0.21378	0.21378	0.00000	0.46402
	Exit	0.78622	0.78622	0.76061	0.00000

Fig. 9.20 Color shift of downlight at 4000 h



2. Color shift after aging (4000 h)

Similarly, we got the view factor table (shown in Table 9.3) for the downlight after aging for 4000 h. Color shift of each individual part and accordingly the color shift of downlight could be calculated. Figure 9.20 shows the color shift of downlight after aging for 4000 h and contribution by each individual part.

9.3.2.4 Comparison and Discussion

Note that color change shown in Figs. 9.19 and 9.20 does not include the color shift of LED packages. Figure 9.21 shows the color shift and contribution of each individual part including LED packages caused by aging.

According to results from the simulation and calculation method, after aging for 4000 h, the downlight has a total color shift of ~0.002, even less than the color shift of LED packages, which is around 0.0025. This is because the two major contributors LED package and diffuser have an opposite contribution in the color shift component of $\Delta v'$. The component $\Delta v'$ of LED package has a decrease of 0.0026, compared to the increase of around 0.0017 caused by diffuser transmission change during aging. Color shift induced by aging of LED packages is quite different from that of diffuser. LED packages' relative flux degradation in SPD occurred obviously in the yellow light area, which induces the color shift to blue. By contrast, the color will shift to yellow for aging of the diffuser since there is much more degradation of flux in the blue light area.

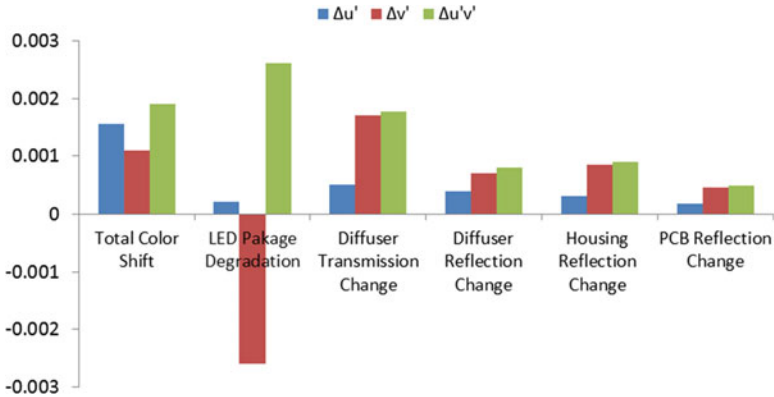


Fig. 9.21 Color shift contribution after aging

Fig. 9.22 Downlight color shift comparison between measurement and proposed approach

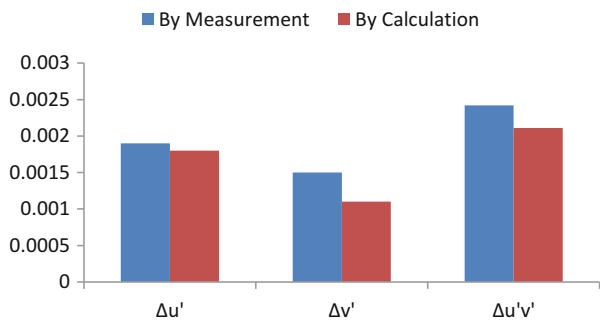


Figure 9.22 shows the comparison between measurement and proposed approach. It could be found that the results are comparable. Errors for the approach proposed in this section could be attributed to several factors. One is the assumption: we assumed there is no bouncing back and forth from LED packages, which would slightly decrease the color change. The other factor is measurement error of optical parameters as inputs for simulation.

9.4 Luminaire Color Shift Acceleration and Prediction

Based on the above investigation, we can breakdown the total color shift $\Delta u'v'$ into component $\Delta u'$ and component $\Delta v'$ for acceleration and prediction. Since each individual part has different contribution and mechanism, we can add up the contribution by each individual part to the color shift component, and acceleration can be performed individually. If we only consider the temperature aging for acceleration, the prediction could be described as below Eqs. 9.9, 9.10, and 9.11.

$$\Delta u'(t, T) = \Delta u'_{\text{led}}(t, T) + \Delta u'_{\text{diffuser}}(t, T) + \Delta u'_{\text{reflector}}(t, T) \quad (9.9)$$

$$\Delta v'(t, T) = \Delta v'_{\text{led}}(t, T) + \Delta v'_{\text{diffuser}}(t, T) + \Delta v'_{\text{reflector}}(t, T) \quad (9.10)$$

$$\Delta u'v'(t, T) = \sqrt{\Delta u'^2(t, T) + \Delta v'^2(t, T)} \quad (9.11)$$

We could follow below steps for luminaire color shift acceleration and prediction.

Step1 For LED packages, determine the SPDs as F (time, temperature) by integrating sphere measurement, and for other components, determine the optical parameters as F (time, temperature) by optics measurement.

Step2 Using Step 1 as inputs, determine the Du' and Dv' as F (time, temperature) for each component by simulation. Meanwhile, determine the view factor matrix as F (time, temperature).

Step3 For each component, fit the acceleration model (linearity, Arrhenius + Weibull/lognormal).

Step4 Calculate system level color shift based on Eqs. 9.9, 9.10, and 9.11.

9.5 Conclusions

In this chapter, we present experimental results for components in LED-based products which have color shift concern. We use this test data as input for a newly developed system level prediction method that we name the view factor approach. We verified the new method with experiments with luminaires to conclude that we have taken satisfactory first step in the field of color shift predictions for LED-based systems.

References

1. Illuminating Engineering Society, *LM-80-08 Standard- Approved Method for Measuring Lumen Maintenance of Led Lighting Sources* (IES, New York, 2008)
2. Illuminating Engineering Society, *TM-21-11 Standard-Projecting Long Term Lumen Maintenance of LED Light Sources* (IES, New York, 2011)
3. China Solid State Lighting Alliance, *CSA-020 Standard-Accelerating Depreciation Test Method for Light Emitting Diode (LED) Lighting Products*, (CSAS, Beijing, 2013)
4. M. Royer, R. Tuttle, S. Rosenfeld, N. Miller, *Color Maintenance of LEDs in Laboratory and Field Applications, Gateway demonstrations, Prepared for Solid-State Lighting Program*, (Wiley, New York, 2013)
5. J. Lynn Davis, K. Mills, M. Lamvik, R. Yaga, S.D. Shepherd, J. Bittle, N. Baldasaro, E. Solano, G. Bobashev, C. Johnson, A. Evans, System reliability for LED-based products, in *15th International Conference on Thermal, Mechanical and Multi-Physics Simulation and Experiments in Microelectronics and Microsystems*, (EuroSimE, Belgium, 2014)

6. Eligibility Criteria – Version 1.3, ENERGY STAR Program Requirements for Solid State Lighting Luminaires., http://www.energystar.gov/ia/partners/product_specs/program_reqs / Solidstate_Lighting_Program_Requirem-nts.pdf
7. W.D. Van Driel, X.J. Fan, *Solid State Lighting Reliability:Components to Systems* (Springer, New York, 2013)
8. S. Chhajed, Y. Xi, Y.-L. Li, T. Gessmann, E.F. Schubert, Influence of junction temperature on chromaticity and color-rendering properties of trichromatic white-light sources based on light-emitting diodes. *J. Appl. Phys.* **97**, 054506 (2005)
9. T. Yanagisawa, T. Kojima, Long-term accelerated current operation of white light-emitting diodes. *J. Lumin.* **114**, 39–42 (2005)
10. L.-R. Trevisanello, M. Meneghini, G. Mura, C. Sanna, S. Buso, G. Spiazzi, M. Vanzi, G. Meneghesso, E. Zanoni, Thermal stability analysis of high brightness LED during high temperature and electrical aging, seventh international conference on solid state lighting, Proc. SPIE. 6669, 666913-3, (2007)
11. J. Huang, D. S. Golubović, S. Koh, D. Yang, X. Li, X. Fan, G.Q. Zhang, Rapid degradation of mid-power white-light LEDs in saturated moisture conditions, *IEEE Trans. Device Mater. Reliab.* **99**, 478–485 (2015)
12. N. Narendran, Y. Gu, J.P. Freyssinier, H. Yu, L. Deng, Solid-state lighting: failure analysis of white LEDs. *J. Cryst. Growth* **268**, 449–456 (2004)
13. J. Huang, D.S. Golubović, S. Koh, D. Yang, X. Li, X. Fan, G.Q. Zhang, Degradation modeling of mid-power white-light LEDs by using Wiener process. *Opt. Express* **23**, A966–A978 (2015)
14. J. Fan, K.C. Yung, M. Pecht, Physics-of-failure-based prognostics and health management for high-power white light-emitting diode lighting. *IEEE Trans. Device Mater. Reliab.* **11**(3), 407–416 (2011)
15. M.H. Chang, D. Das, P.V. Varde, M. Pecht, Light emitting diodes reliability review. *Microelectron. Reliab.* **52**, 762–782 (2012)
16. P. Lall, J. Wei et al, *L70 Life Prediction for Solid State Lighting Using Kalman Filter and Extended Kalman Filter Based Models*, Proceeding ECTC conference Las Vegas USA, (2013) pp. 1454–1465
17. M. Buffolo, C. De Santi, M. Meneghini, D. Rigon, G. Meneghesso, E. Zanoni, Long-term degradation mechanisms of mid-power LEDs for lighting applications. *Microelectron. Reliab.* **55**, 1754–1758 (2015)
18. M. Yazdan Mehr, W.D. van Driel, H. Udono, G.Q. Zhang, Surface aspects of discoloration in bisphenol a polycarbonate (BPA-PC), used as lens in LED-based products. *Opt. Mater.* **37**, 155–159 (2014)
19. M. Yazdan Mehr, W.D. van Driel, K.M.B. Jansen, P. Deeben, G.Q. Zhang, Lifetime assessment of plastics lenses used in LED-based products. *Microelectron. Reliab.* **54**, 138–142 (2014)
20. M. Yazdan Mehr, W.D. van Driel, K.M.B. Jansen, P. Deeben, M. Boutelje, G.Q. Zhang, Photodegradation of bisphenol A polycarbonate under blue light radiation and its effect on optical properties. *Opt. Mater.* **35**, 504–508 (2012)
21. M. Yazdan Mehr, W.D. van Driel, G.Q. Zhang, Progress in understanding color maintenance in solid-state lighting systems. *Engineering* **1**, 170–178 (2015)
22. G. Lu, M. Yazdan Mehr, W.D. van Driel, X. Fan, J. Fan, K.M.B. Jansen, G.Q. Zhang, Color shift investigations for LED secondary optical designs- comparison between BPA-PC and PMMA. *Opt. Mater.* **45**, 37–41 (2015)
23. G. Lu, W.D. van Driel, X. Fan, M. Yazdan Mehr, J. Fan, K.M.B. Jansen, G.Q. Zhang, Degradation of microcellular PET reflective materials used in LED-based products. *Opt. Mater.* **49**, 79–84 (2015)
24. G. Lu, W.D. van Driel, X. Fan, M. Yazdan Mehr, J. Fan, C. Qian, K.M.B. Jansen, G.Q. Zhang, et al., *Opt. Mater.* **54**, 282–287 (2016)
25. G. Lu, W.D. van Driel, X. Fan, M. Yazdan Mehr, J. Fan, C. Qian, G.Q. Zhang, *A POF Based Breakdown Method for LED Lighting Color Shift Reliability* (SSL, China, 2015)
26. G. Lu, W.D. van Driel, J. Fan, C. Qian, H. Ye, X. Fan, G.Q. Zhang, *A Novel Approach for Color Shift Investigation on LED-based Luminaires*, (Eurosim, France, 2016) (On line publication)